Appl Phys B (2010) 98: 797–802
DOI 10.1007/s00340-009-3782-7

Applied Physics B
Lasers and Optics

Resonant cavity based antireflection structures for surface plasmon waveguides

J. Liu · H. Zhao · Y. Zhang · S. Liu

Received: 26 June 2009 / Revised version: 5 September 2009 / Published online: 13 October 2009

Abstract The concept of antireflection coating in the theory of multilayer films is introduced to the two-dimensional metal–insulator–metal (MIM) structures to realize total transmission of optical energy at the waveguide discontinuities. The antireflection structure consists of a resonant cavity which is constructed by changing the insulator width of the waveguide. A numerical method is used to achieve the optimal design directly. A T-splitter with zero reflection is proposed, utilizing a cavity structure in the input waveguide. A transformer with enhanced transmission between different waveguides is presented for further validating the efficiency and generality of these cavity based antireflection structures. The simulation results show that such a structure can realize a perfect antireflection function.

PACS 73.20.Mf · 42.79.Wc · 42.82.Et

1 Introduction

In recent years, there has been much interest in plasmon waveguides because of their outstanding performance in subwavelength optical waveguiding [1–9]. A variety of metallic structures have been proposed as waveguides in nanoscale [10–14]. Among them, the metal–insulator–metal (MIM) waveguide is considered to have unique advantages [13, 14]. It is more compact and easier to integrate into optical circuits compared with the other kinds. To construct a circuit, various basic waveguide components, such as bends [15, 16], splitters [16] and connectors [17], are essential. However, the discontinuities in these structures will cause reflections which will bring about energy loss or even harm the input field. So all these structures demand a negligibly small reflection at the junctions, where energy can be transmitted totally from one waveguide to the others.

Several techniques have been proposed to reduce reflection and enhance transmission in MIM waveguides [15–19]. It has been reported that the high bending transmittance can be obtained by rounding the corner of the bends [15]. Moreover, the results of Veronis and Fan's research [16] show that very efficient right-angle bending and splitting can be realized if the characteristic impedances are matching. For MIM waveguide to waveguide structure, a converter with a power transmission of 86% designed using $\lambda/4$ impedance matching method was proposed in Ginzburg and Orenstein's paper [17]. More recently, Kocabas et al. [18] employed the transmission line and equivalent circuit models and designed a mode converter that can concentrate light from an MIM waveguide of wavelength-sized dimension to one of subwavelength dimension with zero reflection. Matsuzaki et al. [19] introduced the stub structure in microwave engineering to plasmonic circuits and realized a lossless 90° bend in a plasmon waveguide. Xiao et al. [20] employed a resonant cavity at the plasmon waveguides intersection to suppress the crosstalk and promote the throughput. In this paper, in order to increase the transmissions at the waveguide discontinuities, the concept of antireflection coating which is originated from the theory of multilayer films [21] is introduced. The antireflection structure consists of a resonant cavity in the input waveguide to construct a two-layer like structure.

J. Liu · H. Zhao · S. Liu (✉)
Department of Physics, Harbin Institute of Technology,
Harbin 150001, China
e-mail: stliu@hit.edu.cn
Fax: +86-451-86414335

Y. Zhang
Department of Physics, Capital Normal University,
Xisanhuan Beilu 105, Beijing 100037, China

This kind of configuration possesses two advantages: (1) the original structures at the junctions are preserved, and (2) it can be extended to various kinds of waveguide components where reflection exists. In order to achieve optimal results, a numerical method is used for the design directly in this paper.

2 Simplified model for MIM waveguide components

Figure 1 illustrates the two proposed antireflection configurations, which consist of a cavity inside the MIM waveguide with a wider (Fig. 1(a)) or narrower (Fig. 1(b)) insulator. The variable d denotes the insulator width of the original waveguide and d_c is used for the width of the cavity. At the right end of the structure, there is a reflector which may be a bend, splitter or another waveguide in the actual photonic circuits or just free space. In this paper, our study focuses on the modes of propagation in the horizontal (x) direction. Therefore, the metals are presumed to be thick enough in the vertical (y) direction in Fig. 1. For our simulations, the insulator is assumed to be air with a permittivity $\varepsilon_i = 1$. The surrounding metal is silver with a permittivity of $\varepsilon_m = -124.98 + i2.89$ at the wavelength $\lambda = 1550$ nm [22]. Using the dispersion equations it can be demonstrated that only a single propagating mode TM_0 (only $H_z, E_x, E_y \neq 0$) can exist at $d < 0.47\lambda$ for the given ε_m, ε_i and λ [13]. In our structures, the insulator widths of the waveguide and the cavity are all restricted in this range, so that when far from the junctions there is only one propagating mode, since all higher order modes excited at the junctions will decay exponentially with distance. The fundamental TM_0 mode has an insignificant E_x component. Therefore, this mode can be considered as a quasi-TEM mode [16]. Under such circumstances, the cavity structure can be simplified to a 1-D multilayer film structure. Moreover, it can be described as a layered lossless dielectric media structure, which is depicted in Fig. 1(c), if the damping due to the metal is ignored ($\varepsilon_m = -124.98$).

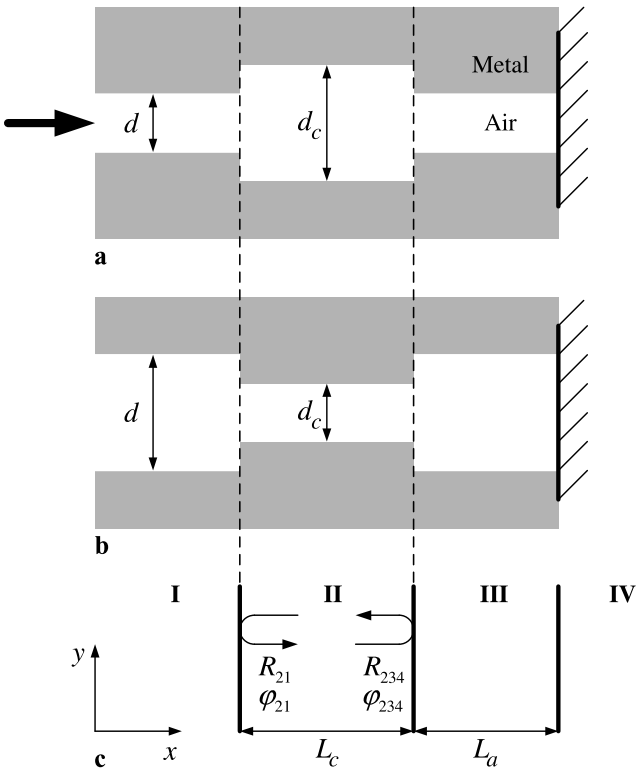

Fig. 1 The schematic diagrams of the antireflection structures with a wider (**a**) or narrower (**b**) cavity and the multilayer films model of these structures (**c**)

Layered antireflection coating is one of the simplest and most widely used structures to achieve the antireflection function in layered dielectric media. In Fig. 1(c) the whole structure can be divided into four parts: part I contains an incident source, part II is a resonant cavity, part III acts as an adjusting layer and part IV is a reflector, respectively. R_{21} and R_{234} denote the energy reflection coefficients at the left and right interfaces of the cavity. φ_{21} and φ_{234} are used for the phase change during the reflection. When the light is illuminated perpendicularly from the incident source I, the reflection can be eliminated in lossless case if the following two conditions are satisfied [18, 21]:

$$R_{21} = R_{234} \quad \text{magnitude condition} \tag{1}$$

$$2k_c L_c + \varphi_{21} + \varphi_{234} = 2m\pi \quad \text{phase condition} \tag{2}$$

where k_c is the propagation constant in horizontal (x) direction in the cavity layer II, L_c is the length of the cavity and m is any integer value. The reflection R_{234} at the right interface of the cavity can be changed continuously by varying the thickness of adjusting layer III. This offers a degree of freedom to match the value of R_{21} and R_{234}. Once the magnitude condition is satisfied, zero reflectance can be achieved by choosing the correct cavity length, which is denoted by L_c in (2).

3 Computation method

Finite-difference time-domain (FDTD) method is used to simulate how the reflections depend on the thickness of the adjusting layer and the cavity layer. Figure 2 describes the steps taken in the calculation of reflection coefficient R in the MIM waveguide when a reflector exists at the end. The reflector could be a bend, splitter or another waveguide with different size, or just free space. Perfectly matched layer (PML) absorbing boundary conditions [23] are used at all boundaries. The FDTD simulation is performed using a uniform Yee cell of $\Delta x = \Delta y = 2$ nm. The propagation mode is excited using a line source with the same

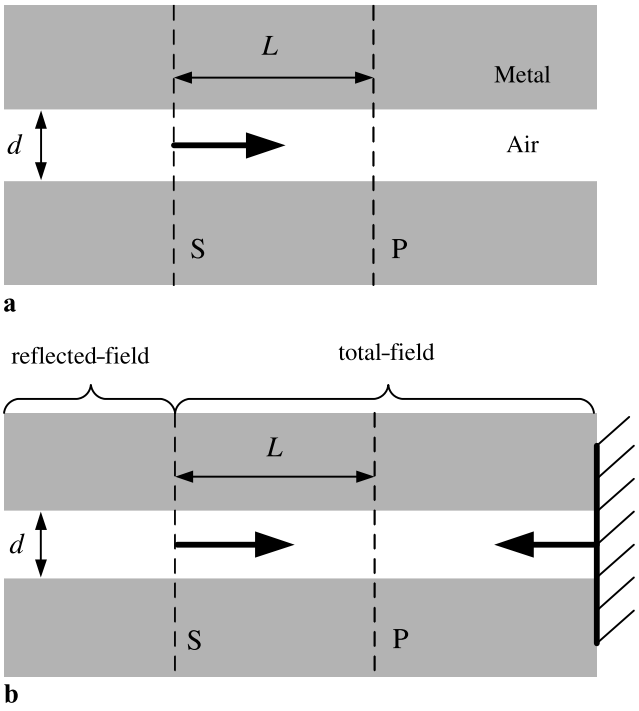

Fig. 2 Description of the steps taken in extracting reflection coefficient R from fields. (**a**) Simulation with a straight waveguide with uniform insulator width. (**b**) A reflector exists at the end of the waveguide. The fields at the plane P in both simulations are recorded and compared to extract the reflection coefficient R. Plane P is set at a distance $L = 200$ nm behind the source plane S

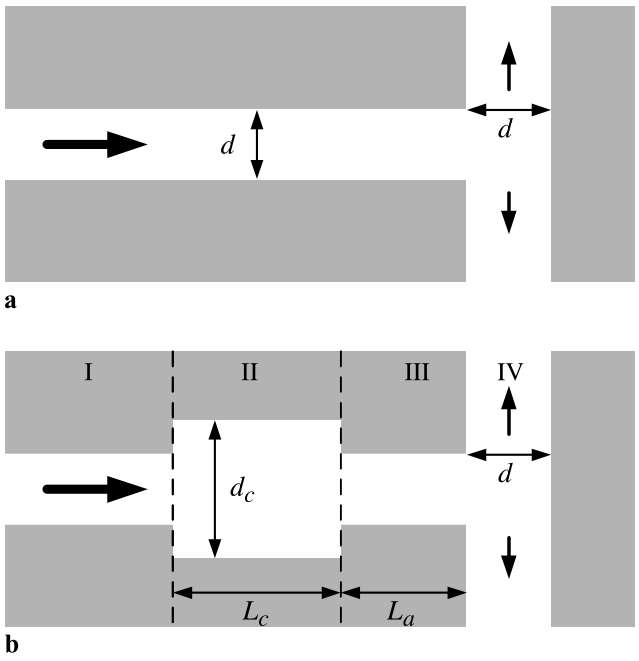

Fig. 3 (**a**) The schematic diagram of a bare T-splitter. (**b**) T-splitter equipped with a cavity as antireflection structure

width as the waveguide at the source plane S, which is depicted in Fig. 2. The power flux of the propagation optical mode is then recorded at plane P, which is about 200 nm away from the source plane. In order to normalize the reflection, the simulation is performed twice, once in the straight waveguide (Fig. 2(a)) and the other with a reflector existing in the waveguide (Fig. 2(b)). By comparing the two cases, the reflection coefficient R can be extracted. To obtain the reflection spectrum, a Gaussian-pulse source can be used instead to cover the desired frequency range and the Fourier transform of the temporal response can be used to extract the spectrum. In order to give an intuitive picture of the reflected field, the incident field at the left-hand side of source plane is canceled in the field evolution process during the FDTD simulation. This configuration divides the problem space into two regions, as illustrated in Fig. 2(b). In the total-field region, field quantities contain the incident and reflected field. The reflected-field region does not contain the incident field.

4 Designs and simulation results

In the following parts of this paper, this kind of antireflection configuration will be employed to reform the tradition waveguide components to validate its efficiency and applicability. One is a modified T-splitter which can transform light into two branches without reflection. The other is a waveguide-waveguide structure which can realize enhanced transmission of light energy from an MIM waveguide with micro-dimension to one with nano-dimension.

4.1 Antireflection for splitters

Splitters, as depicted in Fig. 3(a), are basic structures for optical interconnects and therefore essential components of optical integrated circuits. An ideal symmetrical splitter is presumed to be able to split the light into two equal parts without reflection loss. However, according to the characteristic impedance theory [16], a reflection of 1/9 will be produced at the junction if each branch of the splitter has the same size. For an MIM splitter with insulator width $d = 100$ nm, the energy reflection is 11.91% at 1550 nm wavelength obtained by FDTD method. In this section, we will discuss the cavity structure applied to the T-splitting waveguide to eliminate this reflection.

As discussed above, the whole structure can be divided into four parts as depicted in Fig. 3(b). To realize antireflection, the conditions (1) and (2) must be satisfied. In this paper, d_c is set to be 200 nm. Then, the magnitude condition can be satisfied by varying the thickness of the adjusting layer. The FDTD method is used to calculate the variation of R_{234} with adjusting layer thickness L_a. The results are illustrated in Fig. 4(a). The solid line represents how R_{234} depends on L_a. The dashed line is a reference line which

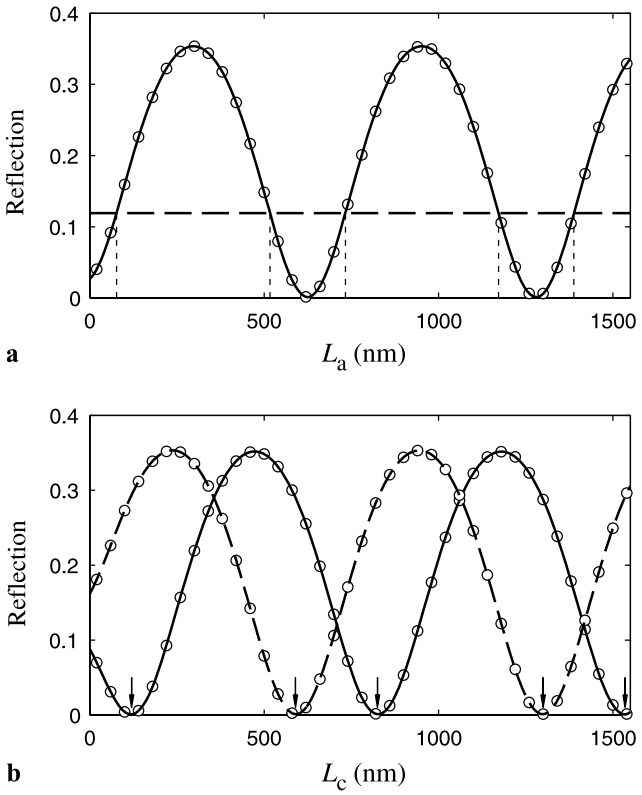

Fig. 4 (**a**) Variation of R_{234} with L_a. The *circles* are the FDTD results. The *solid line* is the numerical fitted curve. The *dashed line* is a reference line representing the value of R_{21}. (**b**) The power reflection of the whole structure with different L_c when L_a is fixed at 77 nm (*solid*) and 517 nm (*dashed*)

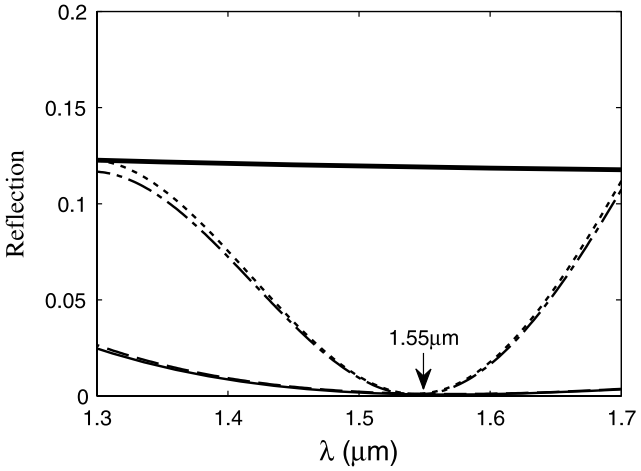

Fig. 5 Reflection spectra of the bare splitter (*thick solid*) and two antireflection splitters with $L_c = 118$ nm, $L_a = 77$ nm (*solid* and *dashed lines* for lossy and lossless cases respectively) and $L_c = 591$ nm, $L_a = 517$ nm (*dash-dot* and *dotted lines* for lossy and lossless cases, respectively)

represents the value of R_{21}. It is clear from the figure that the value of R_{234} is a periodic function of L_a and R_{21} is equal to R_{234} at $L_a = 77$ nm, 517 nm, 733 nm, 1172 nm and 1388 nm.

After L_a is determined, the phase condition (2) can be satisfied by modulating the cavity length L_c. Figure 4(b) illustrates the reflections of the whole structure for different values of L_c at $L_a = 77$ nm (solid line) and 517 nm (dashed line). It is shown that both of the reflections are periodical with the cavity length L_c. From the figure, the reflection is eliminated totally at $L_c = 118$ nm, 827 nm, 1533 nm for $L_a = 77$ nm and $L_c = 591$ nm, 1299 nm for $L_a = 517$ nm, respectively. The intervals are coincident with the analyzed result, $\Delta L_c = 2\pi/(2k_c) = 700$ nm, which is derived from (2). It should also be noticed that the two lines possess the same shape but are mismatched for some space. That is due to the difference of phase change at the right interface of cavity, which is denoted by φ_{234} in (2).

To validate the performance of the designed antireflection structure, the reflection spectrum is calculated by the FDTD method and depicted in Fig. 5. For real metal, the Ohmic loss must be taken into consideration. The lossy case and lossless case are all presented in Fig. 5 for comparison. The thick solid line represents the reflection coefficient for the bare splitter. The thin solid and dash-dot lines represent the reflections of the splitters equipped with antireflection configurations with $L_c = 118$ nm, $L_a = 77$ nm and $L_c = 591$ nm, $L_a = 517$ nm respectively when the Ohmic loss of metal is considered. The lossless cases are also calculated and depicted using dashed and dotted lines in Fig. 5. Compared with a bare splitter, the reflections of the reformed splitters are reduced significantly over a wide bandwidth. From the figure, it is also clear that the antireflection performance of the structure with $L_c = 118$ nm, $L_a = 77$ nm is superior to the other. That is due to the low order resonant mode in the cavity which possesses a flat spectrum compared to the high order ones. The quality factor Q of the cavity, which is associated with the power escape through the waveguide, is proportional to the cavity length [24]. Thus, the lower order resonant mode of the cavity has a lower Q value and therefore broader response which means a flatter spectrum.

To further demonstrate the antireflection function of the proposed structure, the optical field distributions (at 1550 nm wavelength) in the original and modified structures ($L_c = 118$ nm, $L_a = 77$ nm) are calculated by FDTD and displayed in Figs. 6(a) and (b). From the figures, the reflected field is canceled perfectly at the left-hand side of the waveguide. Moreover, in Fig. 6(b), the magnetic intensity is distributed uniformly between source plane S and the waveguide junction, while in Fig. 6(a), there are obvious nodes, which are caused by the interference of the incident and reflected wave. All these results clearly verify that the cavity structure can be used to construct a compact and efficient antireflection T-splitter.

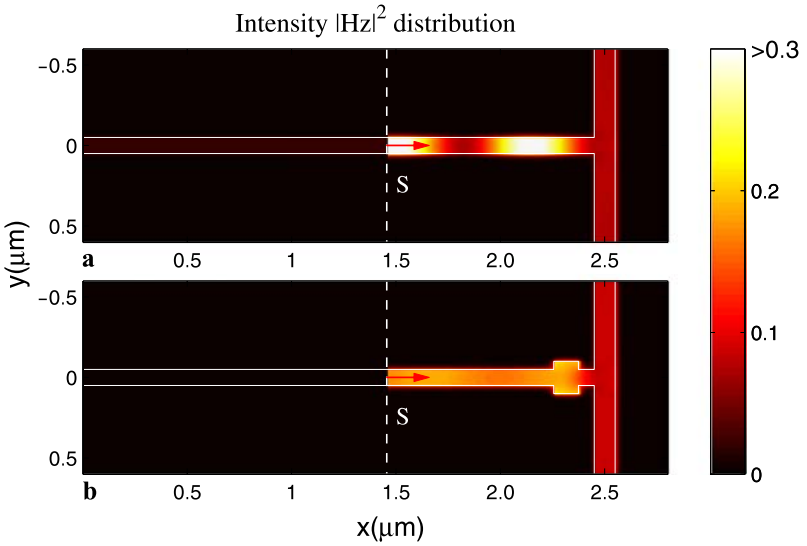

Fig. 6 (**a**) Optical transmission of a bare T-splitter with waveguide width $d = 100$ nm at $\lambda = 1550$ nm. (**b**) Optical transmission when using antireflection configuration

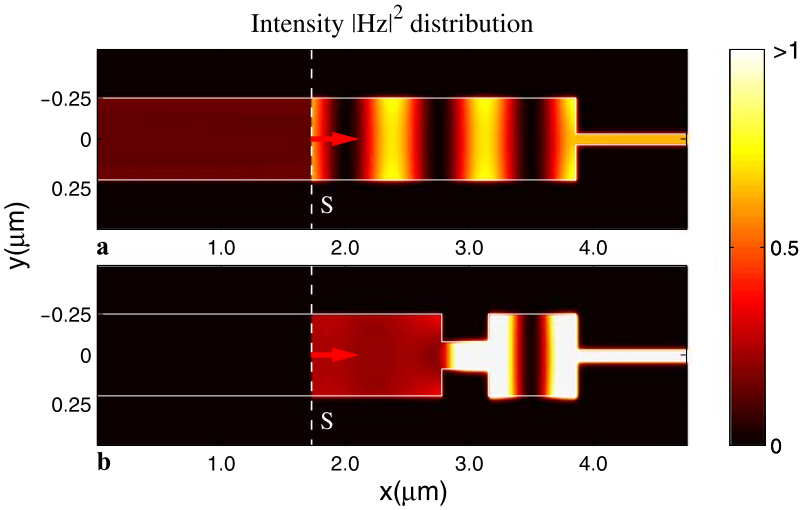

Fig. 7 (**a**) Optical transmission of direct coupling of waveguides from 500 nm to 50 nm. (**b**) Optical transmission when using antireflection configuration

4.2 Antireflection at the junction of different waveguides

In constructing multifunction plasmonic devices, the ability to connect different waveguides is crucial owing to the desire of integrating multiple systems in one chip. In consequence, the unwanted reflections at the junctions should be suppressed as far as possible to realize efficient interaction between different systems. The cavity structures proposed here have the potential to provide such an antireflection function for this kind of connectors. In this section, the cavity based antireflection structure is utilized to concentrate light from an MIM waveguide with insulator width 500 nm to one of 50 nm with zero reflection. Figures 7(a) and (b) show the outlines and the FDTD simulations of the optical transmissions (at 1550 nm wavelength) of the original and modified structures. The same method as above is used to obtain the optimal parameters: $d_c = 150$ nm, $L_c = 388$ nm, and $L_a = 688$ nm. From the figures, the energy is significantly coupled into the 50 nm waveguide when the antireflection structure is added. The reflected field is canceled perfectly in the reflected-field region at the left-hand side of the waveguide. The reflection spectra of the two structures are shown in Fig. 8. The thin solid and dashed line represent the energy reflection of the reformed structure depicted in Fig. 7(b) for the lossy and lossless cases, respectively. The reflections are all suppressed even eliminated around 1550 nm. But for the case of direct coupling, the reflections are all greater than 50% represented by the thick solid line. This result clearly verifies that the cavity structure can be used as a connector to transmit light between waveguides of different dimensions with zero reflection. Moreover, it is also demonstrated that this structure can be extended to various kinds of waveguide components where reflection exists.

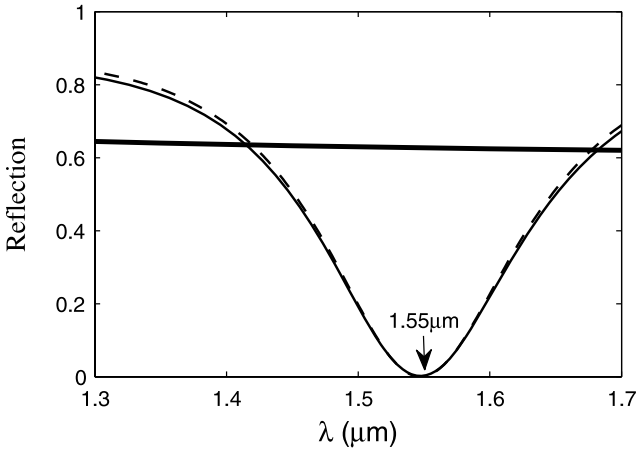

Fig. 8 Reflection spectra of the two structures. The *thin solid* and *dashed line* correspond to the modified structure for lossy and lossless cases respectively. The *thick solid line* represents the reflection spectrum for direct coupling

5 Conclusion

The concept of antireflection coating in the theory of multilayer films is introduced to the two-dimensional MIM structures. An efficient and widely applicable two-layer antireflection structure is proposed. The structure consists of a simple resonant cavity with different width compared to the original waveguide. Two examples are presented to verify its efficiency. One is a T-splitter which can transform light into two branches without reflection. Another one is a waveguide–waveguide structure which can realize enhanced transmission of light energy from an MIM waveguide with micro-dimension to one with nano-dimension. It is expected that the proposed resonant cavity based antireflection structures can bring about a significant advantage for the MIM waveguide based integrated optical circuits.

Acknowledgements This work was supported by the National Natural Science Foundation of China under grants 10674038 and 10604042 and National Basic Research Program of China under grant 2006CB302901.

References

1. T.W. Ebbesen, C. Genet, S.I. Bozhebolnyi, Phys. Today **61**, 44 (2008)
2. S.A. Maier, P.G. Kik, H.A. Atwater, S. Meltzer, E. Harel, B.E. Koel, A.A.G. Requicha, Nat. Mater. **2**, 229 (2003)
3. K. Tanaka, M. Tanaka, Appl. Phys. Lett. **82**, 1158 (2003)
4. G. Veronis, S. Fan, Opt. Lett. **30**, 3359 (2005)
5. L. Liu, Z. Han, S. He, Opt. Express **13**, 6645 (2005)
6. D.F.P. Pile, T. Ogawa, D.K. Gramotven, Y. Matsuzaki, K.C. Vernon, T. Yamaguchi, K. Okamoto, M. Haraguchi, M. Fukui, Appl. Phys. Lett. **87**, 261114 (2005)
7. S.I. Bozhevolnyi, V.S. Volkov, E. Devaux, J.Y. Laluet, T.W. Ebbesen, Nature **440**, 508 (2006)
8. S. Xiao, L. Liu, M. Qiu, Opt. Express **14**, 2932 (2006)
9. R. Zia, M.D. Selker, P.B. Catrysse, M.L. Brongersma, J. Opt. Soc. Am. A **21**, 2442 (2004)
10. D.F.P. Pile, T. Ogawa, D.K. Gramotnev, T. Okamoto, M. Haraguchi, M. Fukui, S. Matsuo, Appl. Phys. Lett. **87**, 061106 (2005)
11. I.V. Novikov, A.A. Maradudin, Phys. Rev. B **66**, 035403 (2002)
12. D.F.P. Pile, D.K. Gramotnev, Opt. Lett. **29**, 1069 (2004)
13. J.A. Dionne, L.A. Sweatlock, H.A. Atwater, Phys. Rev. B **73**, 035407 (2006)
14. E. Feigenbaum, M. Orenstein, J. Lightwave Technol. **25**, 2547 (2007)
15. T.W. Lee, S.K. Gray, Opt. Express **13**, 9652 (2005)
16. G. Veronis, S. Fan, Appl. Phys. Lett. **87**, 131102 (2005)
17. P. Ginzburg, M. Orenstein, Opt. Express **15**, 6762 (2007)
18. S.E. Kocabas, G. Veronis, D.A.B. Miller, S. Fan, IEEE J. Sel. Top. Quantum Electron. **14**, 1462 (2008)
19. Y. Matsuzaki, T. Okamoto, M. Haraguchi, M. Fukui, M. Nakagaki, Opt. Express **16**, 16314 (2008)
20. S. Xiao, N.A. Mortensen, Opt. Express **16**, 14997 (2008)
21. P. Yeh, *Optical Waves in Layered Media* (Wiley, New York, 1988)
22. P.B. Johnson, R.W. Christy, Phys. Rev. B **6**, 4370 (1972)
23. A. Taflove, S.C. Hagness, *Computational Electrodynamics: The Finite-Difference Time-Domain Method*, 2nd edn. (Artech House, Boston, 2000)
24. C. Min, G. Veronis, Opt. Express **17**, 10757 (2009)